

Colloidal indium tin oxide nanoparticles for transparent and conductive films

Young-Sang Cho^a, Gi-Ra Yi^{b,1}, Jeong-Jin Hong^b, Sung Hoon Jang^b, Seung-Man Yang^{a,*}

^a Center for Intergrated Optofluidic System and Department of Chemical and Biomolecular Engineering,
Korea Advanced Institute of Science and Technology, Daejeon 305-701, Korea

^b Corporate R&D Center, LG Chem Research Park, Daejeon 305-380, Korea

Received 26 July 2005; received in revised form 29 June 2006; accepted 11 July 2006

Available online 23 August 2006

Abstract

Nanosized colloidal indium tin oxide (ITO) dispersion was prepared for electrically conductive and transparent coating materials. A titanate coupling agent, isopropyl tri(*N*-ethylenediamino)ethyl titanate, was chosen as a dispersant for the stabilization of ITO nanoparticles in organic solvent. ITO sol was deposited on a cathode ray tube panel for antistatic or electromagnetic shielding purposes, and alkyl silicate was used for the formation of an antireflective over-coat layer. The resulting double-layered coating showed low sheet resistance, which satisfied semi-TCO regulation and low reflectance of visible light. To control the electrical and optical properties of the coating layer, the effects of secondary particle size of ITO aggregates and the dispersant concentration of ITO sol were studied. The stability of ITO sol was estimated by measuring the particle size as a function of the storage days and the aggregation of colloidal ITO dispersion with storage day was explained by depletion flocculation. © 2006 Elsevier B.V. All rights reserved.

Keywords: Antistatic coating; Indium tin oxide; Optical coatings; Reflection spectroscopy; Surface conductivity; Surface morphology

1. Introduction

The international regulations on electromagnetic interference (EMI) caused by electronic or computer devices are progressively becoming stricter so as to protect users from electromagnetic wave. The irradiation of an alternating electric and magnetic fields from video display terminals (VDTs) such as cathode ray tubes (CRTs) is also restricted by some international guidelines or standards. For instance, there are some permissible exposure limits for electric or magnetic fields to prevent harmful effects in human beings from the devices generating electromagnetic fields including VDTs [1]. Since it is possible to shield the emission of electronic wave by increasing the electrical conductivity of the CRT surface, it is necessary to form an electrically conductive and transparent film on the CRT panel [2]. Among the various transparent and conductive oxides for antistatic coating materials, indium tin oxide (ITO) is an attractive material that offers good physical properties [3,4]. Except antistatic or EMI shielding, ITO

thin films can be used for various applications that require both optical transparency in the visible light region and high electrical conductivity, such as electroluminescent devices, electrochromic systems, liquid crystal display electrodes, solar cell and energy efficient windows [5–8].

There are various techniques to deposit ITO film on a substrate surface including chemical vapor deposition, physical vapor deposition, electron beam evaporation and sputtering. However, these methods are not adequate for the mass production of coating films since additional apparatuses such as vacuum equipments are necessary. However, it is possible to form a coating layer with uniform thickness on a substrate having large surface area if a wet-coating method is applied. In this method, a coating solution containing ITO precursors or ITO nanoparticles can be deposited on the substrate by a dip-coating or spin-coating technique [9–12].

The coating film prepared with a coating solution containing ITO powder has a double-layered structure composed of an antistatic (AS) film and an antireflective (AR) over-coat layer. The AS coating solution contains ITO nanoparticles, and the AR coating solution is composed of partially hydrolyzed alkyl silicate. After the polycondensation reaction of silicate during baking of the film, the bonding and fixing of the ITO particles to substrate can be promoted [13]. The reflectance of the film can be reduced in the

* Corresponding author.

E-mail address: smyang@kaist.ac.kr (S.-M. Yang).

¹ Current address: Nano-Bio System Research Team, Seoul Center, Korea Basic Science Institute, 136-713 Korea.

Table 1

Chemical descriptions of various silane or titanate coupling agents used to disperse ITO particles in organic medium and the sedimentation test results

Chemical description	ITO (wt.%)	Coupling agent (wt.%)	Sedimentation ratio (% , after 9 days)	Secondary particle size of ITO dispersion (nm)
3-(Trimethoxy silyl)propyl methacrylate	15	0.67	77.0	392.3±5.8
<i>N</i> -[3-(Trimethoxy silyl)propyl]ethylenediamine	15	0.67	0.5	86.2±6.6
Isopropyl tri(<i>N</i> -ethylenediamino)ethyl titanate	15	0.67	0.0	85.1±3.2
Neopentyl(dialyl)oxy tri(<i>N</i> -ethylenediamino)ethyl titanate	15	0.67	1.9	148.7±6.9
Isopropyl tri(dioctyl)pyrophosphato titanate	15	0.67	38.1	433.1±59.6
Di(dioctyl)pyrophosphate oxoethylene titanate	15	0.67	43.8	627.6±34.6

presence of an over-coated AR layer to promote destructive interference of incident light onto the CRT panel [14].

In order to disperse ITO particles in the coating solution, it is necessary to stabilize the ITO suspension in an organic solvent. A stable colloidal dispersion of metal oxides can be prepared by an electrostatic or steric stabilization method. The repulsive force from the electric double layer on the surface of the colloidal particles can be used to avoid particle aggregation [15]. Meanwhile, the steric barrier formed by the adsorbed surfactant to render osmotic repulsive force between the colloidal particles can prevent the colloidal dispersion from flocculating [16]. For the case of ITO dispersion, steric stabilization is more desirable since the zeta potential of ITO powder is quite small (usually less than 20 mV in organic medium). Thus, a suitable stabilizing agent should be selected to prepare a stable ITO suspension. However, high molecular weight surfactants such as polymeric dispersants are not suitable since the adsorbed polymers can act as an insulating layer to reduce the electrical conductivity of the film. Since titanate or silane coupling agent with relatively small molecular weight can adsorb on the surface of metal oxide, they can be used as a stabilizing agent for the ITO coating solution [17].

In this paper, we report the application of a dispersion technique for the formation of antistatic coating. Various kinds of titanate or silane coupling agents were tested to select a desirable stabilizing agent of the ITO dispersion for CRT coating. Factors affecting dispersion stabilization of ITO sol and the physical properties of the coating film were studied. The AS and AR coating solutions were deposited on a CRT panel by a spin coater, and the electrical and optical properties were measured for the ITO film in order to assess the physical properties of the coating layer. Finally, the long-term stability of the ITO dispersion was studied by measuring the secondary particle size as a function of the storage time.

2. Experimental details

2.1. Materials

Commercially available ITO nanopowder manufactured by SinoTech Co., Ltd. was used as ultrafine particles suspended in the coating solution. A mixture of ethanol (Merck, 99.9%), DMF [*N,N*-dimethylformamide, HCON(CH₃)₂, Duksan Pharmaceutical Co., 99.9%] and IPC (2-isopropoxyethanol, Aldrich, 99.9%) was used as a dispersion medium. The dispersants listed in Table 1, which were used as dispersion stabilizers for ITO sol, were purchased from Kenrich Petrochemicals except 3-(trimethoxy silyl)

propyl methacrylate and *N*-[3-(trimethoxy silyl)propyl]ethylenediamine which was purchased from Aldrich. ZrO₂ beads with 0.3 mm in diameter (Chunwoo Material Co.) were used to re-disperse ITO aggregates in dispersion medium during the milling process.

2.2. Powder characterization

The morphology of ITO particles was observed by Energy Filtering Transmission Electron Microscopy (EF-TEM, EM912 Omega). The sample was prepared for observation by mixing ITO powder with ethanol followed by sonication. A drop of the ITO dispersion was then placed onto a standard microscope grid coated with copper film. After evaporation of the solvent, the morphology of the sample was observed.

The crystallinity of ITO powder was assessed from powder X-ray diffraction (XRD) patterns. XRD measurement was performed on a Rigaku D/MAX-RC apparatus. The incident wavelength was Cu K α =0.154056 nm and the detector was moved between $2\theta=15^\circ$ and 75° . The scan speed was $3^\circ/\text{min}$.

The specific surface area of the ITO particle was measured by BET (Brunauer-Emmet-Teller) method. The chemical composition of the ITO particle was measured by WDS (Wavelength Dispersive Spectrometer, Electron Probe X-ray Microanalyzer, JXA 8900R) technique.

2.3. The selection of dispersant for stable ITO sol

Colloidal suspension of ITO was prepared by dispersing 15 wt.% of ITO powder in organic solvent. Various kinds of titanate or silane coupling agents listed in Table 1 were dissolved in ethanol by stirring for two hours with a magnetic stirrer. The mixture of ITO powder and solvent was contained in a 125 mm bottle made of polypropylene, and the diluted dispersant solution was added to the bottle. The typical composition of the dispersion medium was 0.67 wt.% of coupling agent, 74.5 wt.% of ethanol, 3 wt.% of DMF and 7.5 wt.% of IPC. In order to redisperse aggregated ITO particles in dispersion medium, 50 ml of ZrO₂ beads with 0.3 mm in diameter was added to the bottle, and the attrition of ITO particles was performed by a vibratory milling machine. The milling machine used in this study was a paint shaker purchased from Red Devil Equipment Co. Ltd. (5400 series, Y3 model, 670 rpm).

In order to observe the macroscopic stability of ITO sol, settling experiments were performed for each ITO sol dispersed by different coupling agents. These experiments were performed

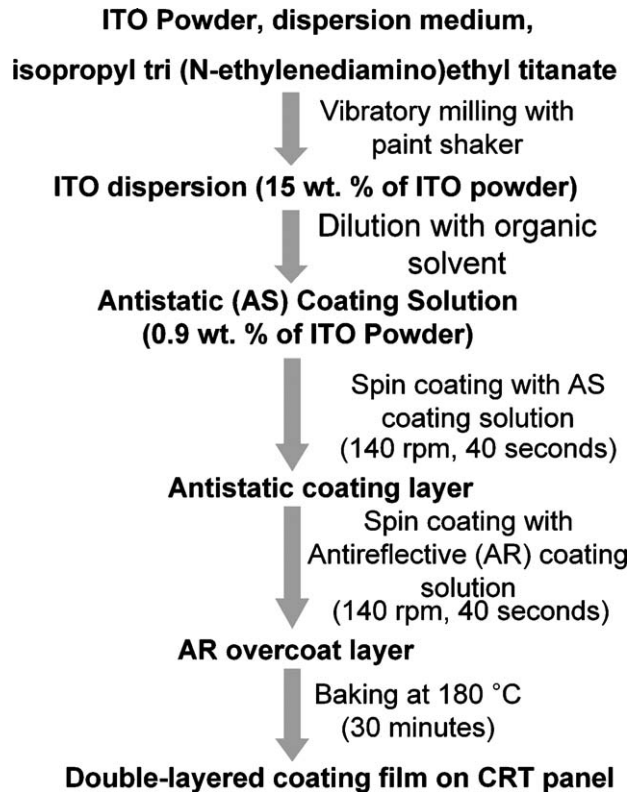


Fig. 1. Experimental procedure for the antistatic and antireflective coating of the cathode ray tube panel with colloidal indium tin oxide dispersion and partially hydrolyzed alkyl silicate solution.

with 10 ml mass cylinders filled with ITO sol comminuted for 8 h. Immediately after attrition for 8 h, the secondary particle sizes of colloidal ITO dispersions were measured by dynamic light scattering (DLS). DLS measurements were performed with ZETA PLUS equipment (Brookhaven instrument) at a wavelength of 674 nm at 90° incident angle to measure the secondary particle size of the ITO sol.

So as to avoid the evaporation of dispersion medium, the top of the mass cylinder was sealed with rubber and paraffin film. The initial heights of the ITO sol in the mass cylinder and settling height of the ITO particles were measured after 9 days since the sample preparation. The sedimentation ratio of ITO sol was then calculated according to the following Eq. (1).

$$\text{sedimentation ratio} = 1 - \frac{\text{settling height of particles}}{\text{initial height of ITO sol}} \quad (1)$$

The sedimentation results using various dispersants are summarized in Table 1.

2.4. Adsorption isotherm of dispersant on the surface of ITO particles

The adsorption isotherm of the dispersant used to stabilize the ITO suspension was obtained by EA (elemental analysis). Various amounts of dispersant were added to the ITO sol to stabilize 15 wt.% of ITO suspension and agglomerated ITO particles were comminuted by vibratory milling machine for

4 h. Ethanol was used as the only solvent consisting of a dispersion medium and was separated from ITO particles by centrifugation (12,000 rpm, 6 h). The centrifuged ITO particles were dried in a convection dry oven at 60 °C, and the surface elemental composition of the dried powder was analyzed by EA to determine the adsorbed amount of dispersant. The amount of elemental nitrogen on the ITO particles measured by EA was converted to the adsorbed moles of dispersant, isopropyl tri(*N*-ethylenediamino)ethyl titanate, considering the BET surface area of the ITO powder.

2.5. Preparation of ITO coating layer on CRT panel

The procedure of the coating and baking of ITO film is shown in Fig. 1. To deposit a coating film on a 17-in. CRT panel, ITO sol stabilized by isopropyl tri(*N*-ethylenediamino)ethyl titanate was diluted and AS coating solution was prepared. The amount of ITO in the AS solution was 0.9 wt.%. Before the deposition of the AS film, the surface of the CRT panel was washed with diluted aqueous hydrofluoric acid solution and dried by an air blower so as to remove dust on the panel. The CRT panel was then heated to 50 °C in a convection dry oven and cooled to 43 to 44 °C by washing with ethanol followed by the deposition of the AS coating film. After the antistatic coating was finished, an AR coating solution composed of alkyl silicate was deposited over the AS coating layer. Both the AS and AR coatings were prepared using a spin coater. The rotating speed of the CRT panel during the spin-coating processes was 140 and 160 rpm for AS and AR coatings, respectively, and the rotating duration of the spin coater was 40 and 35 s for AS and AR coating, respectively. The coated CRT panel was subsequently baked at 180 °C for 30 min in order to evaporate the solvent from the AR coating layer and to facilitate the formation of a silica layer. The cross-sectional image of double-layered coating film was taken with environmental scanning electron microscope (E-SEM, LEO 1455VP).

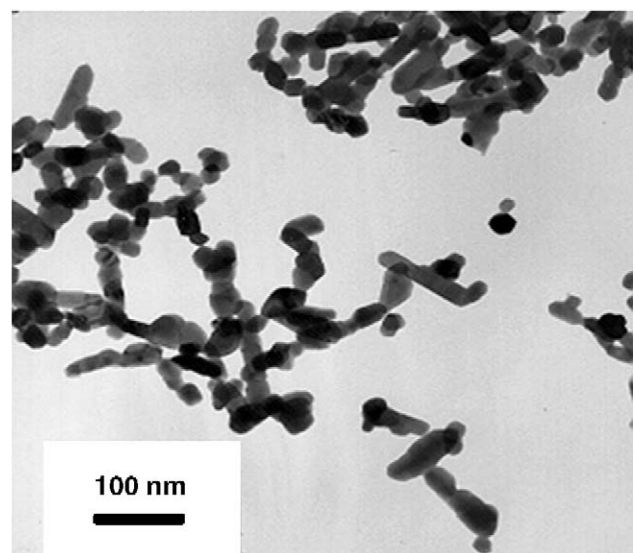


Fig. 2. TEM image of commercialized indium tin oxide powder purchased from SinoTech. Scale bar is 100 nm.

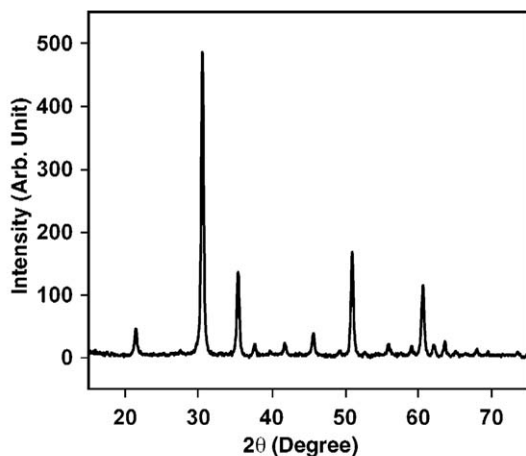


Fig. 3. X-ray diffraction pattern of commercialized ITO powder purchased from SinoTech.

2.6. Measurement of electrical and optical properties of coating film

The sheet resistance was measured by a four-probe technique with a Loresta HP (MCP-T410, Mitsubishi Chemical). The visible light reflectance of the coating layer was measured by a Darsa Pro-5000 System (Professional Scientific Instrument).

3. Results and discussion

The morphology of the ITO powder is shown in Fig. 2. As noted, the primary particles of ITO powder had spherical or ellipsoidal shape. The rod-like morphology of some particles in Fig. 2 may be caused by the aggregation of primary particles. Fig. 2 shows crystalline particles with an average size of 20 to 30 nm.

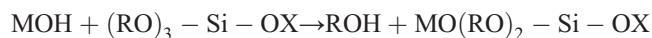
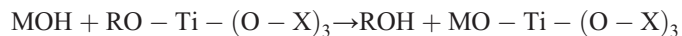
The X-ray diffraction patterns of the ITO powder are shown in Fig. 3. These patterns coincide well with that of indium oxide, but with slight deviation from that of genuine indium oxide. Since there was no diffraction in the spectrum of tin oxide, the ITO powder used in this study has an indium oxide cubic bixbyite crystal structure without any tetragonal tin oxide domain [18]. From the XRD result, the primary particle size can be determined from Scherrer's formula [19]. The calculated primary particle size of the ITO powder was 22.02 nm, which is consistent with the particle size measurement obtained from the TEM image.

The tin doping ratio, $\text{Sn}/(\text{Sn}+\text{In})$, of ITO powder obtained by WDS technique was measured as 8.64 at.%. Notably, the carrier density of ITO increases almost linearly with increasing tin doping ratio up to about 8 at.% and then saturates at higher doping concentrations [20]. Thus, it is implied that the tin doping amount of ITO powder used in this study is almost optimized in terms of maximum electrical conductivity.

The specific surface area and pore volume of ITO powder measured by BET method were $30.33 \text{ m}^2/\text{g}$ and $0.214 \text{ cm}^3/\text{g}$, respectively, indicating that the particles have low porosity.

We have used various titanate or silane coupling agents as dispersants listed in Table 1 to prepare stable ITO dispersions.

Since the alkoxy group of the coupling agent is highly reactive with the surface hydroxyl group of ITO particles, the coupling agent can adsorb on the ITO surface. The possible chemisorption mechanism of titanate or silane coupling agent can be represented as the following alcoholysis reaction [21].



In the above expression, MO denotes metal oxide, and RO and X stand for the alkoxy and binder functional group of the coupling agent, respectively. Thus, the alkoxy group of the coupling agent can act as an anchoring part on the powder surface. The other functional group X can be a grafted segment to render steric repulsion in a strongly interacting solvent.

Table 1 shows the secondary particle size and the result of sedimentation test for the ITO dispersions obtained after 9 days since the sample preparation. The amount of ITO particles and dispersant in dispersion medium were fixed as 15 wt.% and 0.67 wt.%, respectively. As shown in Table 1, the ITO sol dispersed by isopropyl tri(*N*-ethylenediamino)ethyl titanate did not show a clear boundary between liquid medium and settled particles. In this case, green ITO sol was obtained without any precipitates. However, ITO sols which were dispersed by the remaining coupling agents settled down, and clear supernatant over the sedimented ITO aggregates was observed during sedimentation test. Moreover, when the secondary particle size of ITO dispersion was larger than 400 nm, large fluctuation of measured particle size was observed as shown in Table 1. The relatively small size of the isopropyl group and the strong affinity of the ethylene diamino group to the dispersion medium enhanced the stabilizing effect of isopropyl tri(*N*-ethylenediamino)ethyl titanate. However, flocculation of the ITO dispersion was observed when coupling agents have a bulky alkoxy group such as neopentyl(dialyl)oxy tri(*N*-ethylenediamino)ethyl titanate. The particle aggregation was also observed

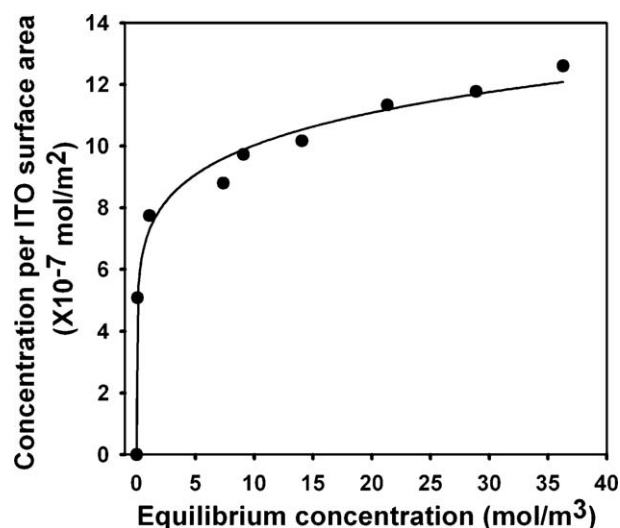


Fig. 4. Adsorption isotherm of tri(*N*-ethylenediamino)ethyl titanate on the surface of indium tin oxide nanoparticles.

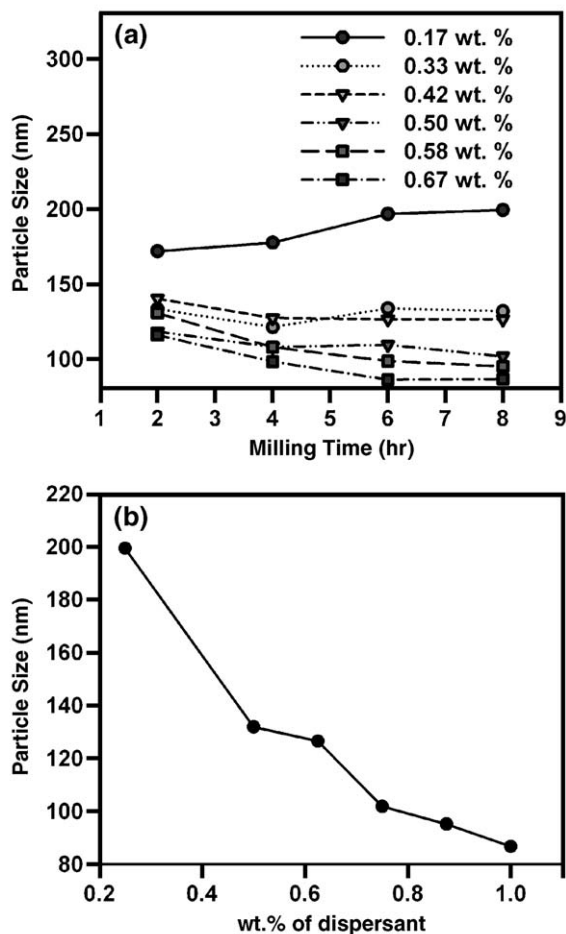


Fig. 5. (a) Secondary particle size of colloidal indium tin oxide dispersion as a function of the dispersant concentration and milling time. Tri(*N*-ethylenediamino)ethyl titanate was used as dispersant. (b) The secondary particle size of colloidal indium tin oxide dispersion as a function of the dispersant concentration after 8 hour of vibratory milling. Tri(*N*-ethylenediamino)ethyl titanate was used as dispersant.

when the number of binder functional groups per coupling agent was less than three or when methacrylate or a phosphate group was contained in the binder functional group. Insufficient number of grafted chains or weak affinity of the coupling agent with organic medium may be responsible for the flocculation of ITO dispersion. Even though the effect of *N*-[3-(trimethoxy silyl)propyl]ethylenediamine on the secondary particle size of ITO sol was similar to that of isopropyl tri(*N*-ethylenediamino)ethyl titanate, slight sedimentation of ITO dispersion was observed when *N*-[3-(trimethoxy silyl)propyl]ethylenediamine was used as dispersant as shown in Table 1. Considering these factors, isopropyl tri(*N*-ethylenediamino)ethyl titanate was selected as the best stabilizing agent for ITO sol.

The adsorption isotherm was obtained to study the adsorption behavior of isopropyl tri(*N*-ethylenediamino)ethyl titanate on ITO powder. Fig. 4 shows the adsorption concentration of the dispersant with equilibrium concentration in the solvent phase. This isotherm was similar to a Langmuir type, implying highly energetic adsorption at a low surface concentration [15]. According to this result, the adsorption

concentration begins to saturate when the equilibrium concentration is about 7.4 mol/m^3 .

Fig. 5(a) shows the secondary particle size of ITO sol measured as a function of the milling time for various concentrations of dispersant, isopropyl tri(*N*-ethylenediamino)ethyl titanate. The concentration ranged from 0.17 to 0.67 wt.% of isopropyl tri(*N*-ethylenediamino)ethyl titanate based on the weight of ITO. The milling was continued for 8 h. Since the ITO powder readily aggregates in an organic solvent, it is necessary to comminute aggregated ITO particles by inflicting collision energy in addition to using a stabilizing agent. This can be realized by various kinds of milling machines. In a laboratory scale, a batch type vibratory milling machine such as a paint shaker is ideal, and the aggregated ITO particles can collide with ZrO_2 beads to be comminuted. Using this apparatus, stable ITO sol can be obtained within a few hours of milling time. As shown in Fig. 5(a), the secondary particle size decreases with the milling time due to the attrition of aggregated ITO particles with ZrO_2 beads. Fig. 5(b) shows the secondary particle size of ITO sol after 8 h of milling. From this figure, it can be seen that the secondary particle size was decreased as the amount of dispersant was increased. As the dispersant concentration decreases, the number of grafted dispersant molecule on the ITO surface decreases. Thus, the steric repulsion would also decrease and the particles will aggregate due to van der Waals force. When the dispersant concentration was less than 0.45 wt.%, the secondary particle size could not be reduced to less than 120 nm even after 8 h of vibratory milling.

Fig. 6 shows the cross-sectional scanning electron micrograph of double-layered ITO/silica coating layer on CRT glass panel. Under the spin-coating conditions described in Fig. 1, the thickness of ITO coating layer is ca. 80 nm, which is the secondary particle size of ITO sol approximately, as can be seen from Fig. 6. The over-coat silicate film (AR layer) on ITO coating film (AS layer) can be also clearly confirmed from Fig. 6.

Fig. 7(a) represents the schematic of the model for the electrical resistance of ITO coating film. The electrical resistance of the ITO film arises from three factors—the resistance of the ITO aggregate (specific resistance, R_s), the resistance of the adsorbed surfactant layer (surface adsorption resistance, R_i) and

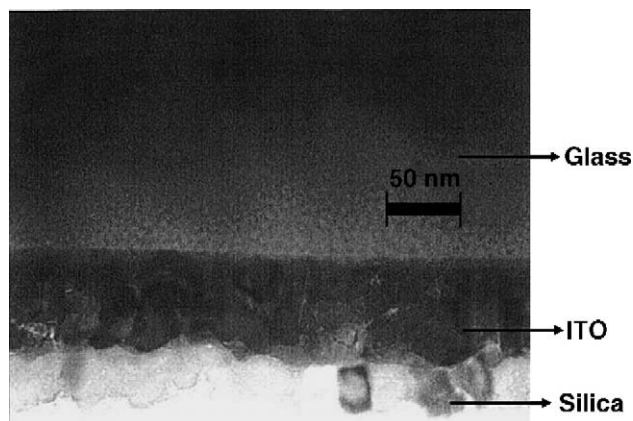


Fig. 6. Scanning electron micrograph of double-layered indium tin oxide/silica coating layer. Scale bar is 50 nm.

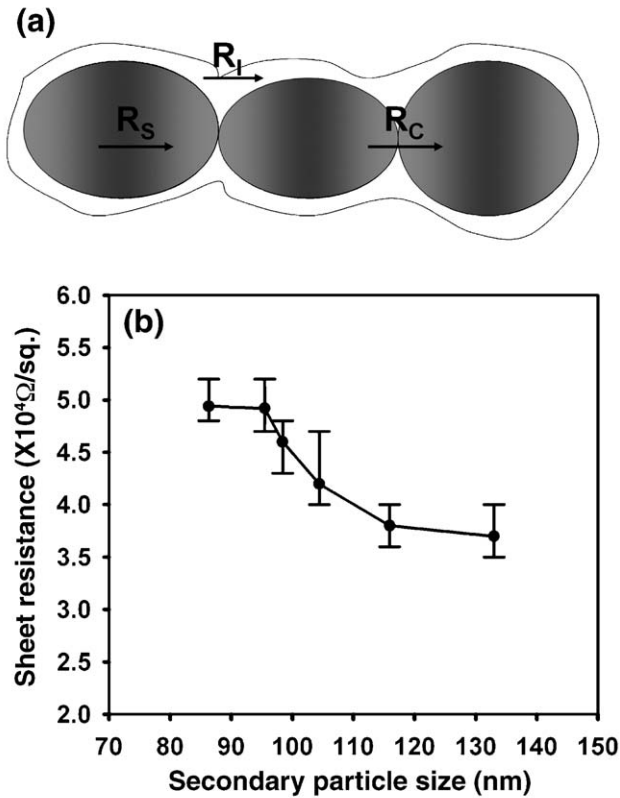


Fig. 7. (a) The schematic of the model for the electrical resistance of ITO coating film. (b) Sheet resistance of coating film as a function of the secondary particle size of colloidal indium tin oxide dispersion (antistatic coating solution). Error bars indicate the variation of sheet resistance depending on the position of CRT surface.

the resistance due to the contacting area between ITO aggregates (contact resistance, R_c). The overall resistance of the coating film R_o can be represented as Eq. (2)

$$\frac{1}{R_o} = \frac{1}{R_s + R_c} + \frac{1}{R_l} \quad (2)$$

The specific resistance can be decreased during the preparation step of ITO powder by changing the tin doping ratio or reduction condition during the preparation step of ITO powder [22]. On the contrary, the other two factors can be improved during the preparation step of the ITO dispersion by adjusting the secondary particle size of the ITO sol or the amount of dispersant.

In order to study the effect of secondary particle size on the electrical properties of the coating layer, the sheet resistance of the coating film was measured with different sizes of ITO aggregates. The results are shown in Fig. 7(b). As the particle size of ITO decreases, density of ITO aggregates increases. Thus, the electrical conductivity of the coating film decreases due to the increase of contact resistance. When the milling process lasts longer than 7 h, exact measurement of sheet resistance was difficult due to the increased electrical resistance. The measured sheet resistance of the coating film ranged from 3.7 to $5.5 \times 10^4 \Omega/\square$ satisfying semi-TCO regulation.

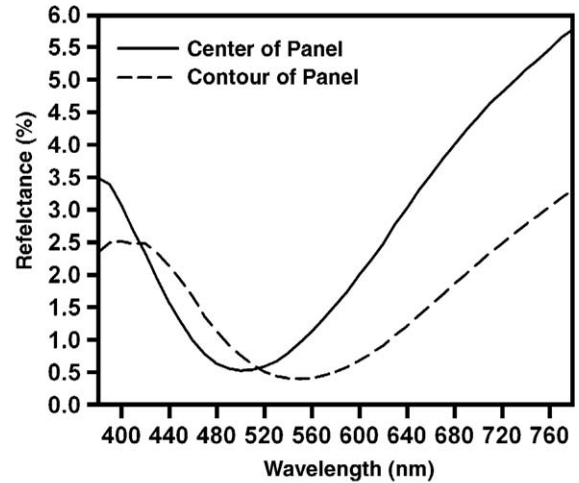


Fig. 8. Visible light reflectance of cathode ray tube panel as a function of the wavelength of incident light. The secondary particle size and dispersant concentration of colloidal indium tin oxide dispersion are 101 nm and 0.67 wt.%, respectively.

Fig. 8 shows the typical visible light reflectance of the AS and AR coating layer as a function of the wavelength of incident light. According to this figure, the antireflective effect is dependent on both the wavelength of incident light and the measured position on the CRT surface. Compared to the central part of the CRT panel, the minimum reflectance corresponds to longer wavelength on the contour part of the panel. During the spin-coating process, coarse particles spread far from the center of the panel due to centrifugal force acting on the particles, resulting in a particle size distribution along the distance from the center of the panel. This distribution is responsible for the position dependent optical property of the coating layer shown in Fig. 8. The wavelength corresponding to the minimum reflectance was observed near 555 nm. Because the human eye

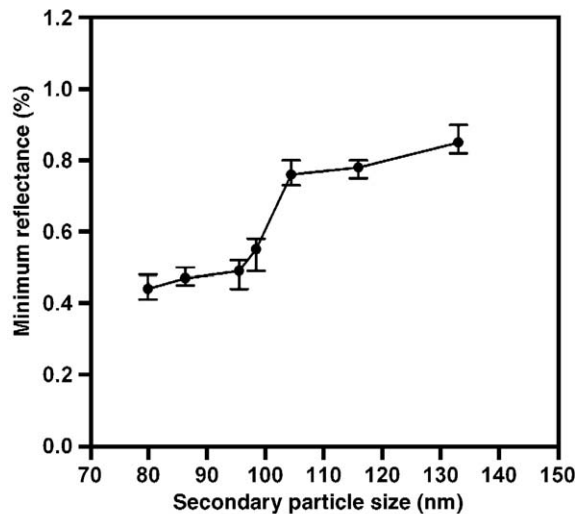


Fig. 9. Minimum reflectance of coating film as a function of the secondary particle size of colloidal indium tin oxide coating solution (antistatic coating solution). Error bars indicate the variation of minimum reflectance depending on the position of CRT surface.

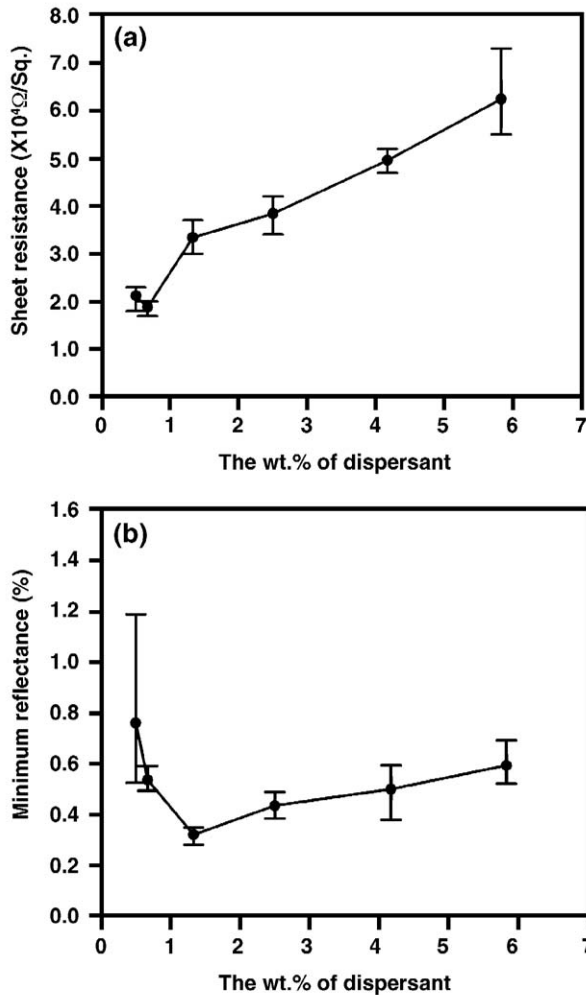


Fig. 10. (a) Sheet resistance of coating film as a function of the dispersant concentration of colloidal indium tin oxide dispersion. Error bars indicate the variation of sheet resistance depending on the position of CRT surface. (b) Minimum reflectance of coating film as a function of the dispersant concentration of colloidal indium tin oxide dispersion. Error bars indicate the variation of minimum reflectance depending on the position of CRT surface.

is the most sensitive to 555 nm, which corresponds to the color green, low reflectance near this wavelength is sufficient for the antireflective property of the CRT coating layer.

The optical property of the transparent coating can be assessed by measuring the reflectivity, which can be expressed by Eq. (3) [23].

$$R = \left[\frac{n_1^2 n_s - n_2^2 n_a}{n_1^2 n_s + n_2^2 n_a} \right]^2 \quad (3)$$

Here, R is the reflectivity corresponding to the film thickness, which is a quarter of the wavelength of the light, and n_a , n_s , n_1 and n_2 are refractive indices of air, CRT panel, and the AR and AS coating layer, respectively. Since the refractive indices of air and the CRT panel are 1.00 and 1.54, respectively, the condition of minimizing reflectivity is $n_2 = 1.24n_1$. Thus, lower reflectance can be obtained by increasing the refractive index of the AS coating layer.

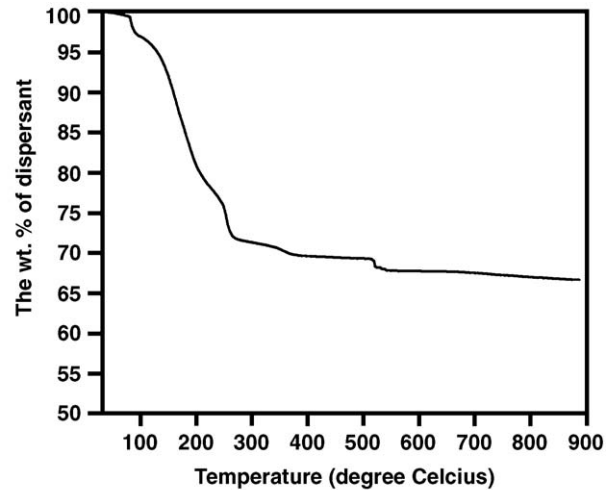


Fig. 11. Thermogravimetric analysis of dispersant (isopropyl tri(*N*-ethylenediamino)ethyl titanate).

Fig. 9 shows the minimum reflectance of the coating film deposited with ITO sol. As the particle size of ITO aggregates in the film increases, the void space between ITO particles will be filled by a greater amount of AR solution, resulting in a decreased refractive index of the AS coating layer (the refractive index of ITO is ca. 2). Thus, the reflectance of the coating layer increases as the particle size of the ITO sol increases, as shown in Fig. 9. Whitening of the coating film was observed when the secondary particle size of the ITO sol was larger than 130 nm, due to coarse particles in the ITO sol. Thus, the critical particle size to cause whitening was determined as 130 nm. The coating film showed excellent optical transparency when the particle size of ITO sol is less than this critical value.

Fig. 10(a) and (b) show the sheet resistance of the ITO coating film and the minimum reflectance of the coating layer as a function of the amount of dispersant used to stabilize the ITO sol, respectively. To exclude the effect of particle size, the secondary particle size of the ITO sol was adjusted to 101 ± 3.7 nm. The amount of dispersant was based on the weight of the ITO powder. In Fig. 10(a), the sheet resistance of the film increases drastically

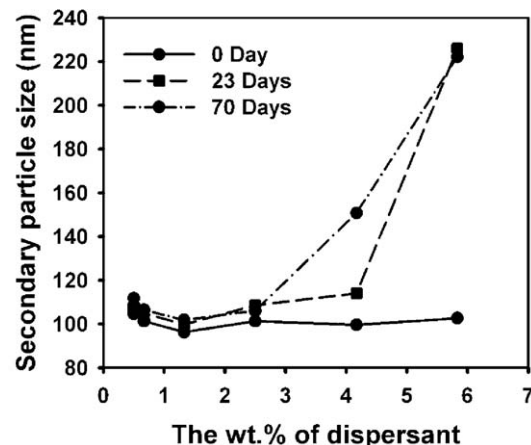


Fig. 12. Change of secondary particle size of colloidal indium tin oxide dispersion with wt.% of dispersant and storage day.

with an increasing amount of dispersant since the adsorbed layer of the dispersant on the ITO surface acts as an insulating layer. This is clearly confirmed by the thermogravimetric analysis (TGA) of isopropyl tri(*N*-ethylenediamino)ethyl titanate shown in Fig. 11. According to the TGA result, more than 85% of the dispersant will remain after baking of the coating panel at 180 °C resulting in a decrease of conductivity of the ITO film.

In Fig. 10(b), the dependence of the optical property on the amount of dispersant is not significant, unlike the electrical property of the coating film. However, the appearance of the coated surface was damaged severely when the amount of dispersant increased. With an increasing amount of dispersant in the AS coating solution, the unadsorbed dispersant that remains in the solvent phase can spread on the surface of the panel during the spin-coating process. This presumably caused the scratched pattern that was observed on the surface of the CRT panel when an excessive amount of dispersant was used.

For commercial use of ITO sol, the long-term stability of the colloidal dispersion should be guaranteed for at least two months. Thus, ITO sol was prepared by varying the amount of dispersant and the secondary particle size was measured as a function of the storage time. During these measurements, ITO sol was stored in a refrigerator at 4 °C. Fig. 12 shows an increase of secondary particle size after several storage days. When the amount of dispersant was less than 4.2 wt.%, the aggregation of ITO particles was negligible. On the contrary, severe particle aggregation was observed when more than 4.2 wt.% of dispersant was used. This is because the unadsorbed dispersant dissolved in the dispersion medium can cause the attractive osmotic pressure to aggregate ITO particles through depletion flocculation.

It is generally accepted that non-adsorbed dispersant may promote the flocculation of a colloidal system via depletion flocculation. Non-adsorbed dispersant will alter their configuration if their center of mass approaches to the surface at a distance that is less than its Flory radius [24]. In this case, a depletion layer is formed, where the dispersant concentration decreases toward the particle surface. When the depletion layers of two particles overlap, dispersant will be excluded and the osmotic pressure becomes unbalanced, resulting in particle attraction. This depletion flocculation occurs when an excessive amount of dispersant is used. We have confirmed that the ITO dispersion also displays this behavior when an excessive amount of dispersant was used.

4. Summary and conclusions

Colloidal solution of ITO was prepared by milling ITO powder together with isopropyl tri(*N*-ethylenediamino)ethyl titanate as a dispersant in organic solvent. The adsorption behavior of the dispersant on the surface of the ITO powder was Langmuir-type, implying strong affinity of the adsorbate and adsorbent. The ITO dispersion was deposited on the CRT panel to increase the surface conductivity of the CRT, and alkyl silicate was used for the formation of an antireflective over-coat layer. The double-layered coating film showed a low minimum reflectance of about 1% and a sheet resistance of the order of $10^4 \Omega/\square$, which was enough to satisfy antireflective and antistatic properties. The electrical

resistance and visible light reflectance of the coating film were affected by the secondary particle size of the ITO dispersion. Larger particle size of ITO decreased the sheet resistance due to a decrease of contact resistance between ITO aggregates, but increased the visible light reflectance due to the lowered refractive index of the AS coating layer. The CRT panel appeared white when the particle size of the ITO aggregates was larger than 130 nm, due to the scattering by the coarse particles. The electrical property was also affected by the concentration of the dispersant, which acts as an insulating layer on the surface of ITO aggregates. The amount of dispersant also affected the long-term stability of the ITO dispersion due to depletion flocculation, providing the upper limit of dispersant concentration of the ITO sol.

Acknowledgment

This work was supported by a grant from the Creative Research Initiative Program of MOST/KOSEF for “Complementary Hybridization of Optical and Fluidic Devices for Integrated Opto-fluidic Systems.” We would like to express our gratitude for partial support for this research by the BK21 Project of Korea and CUPS-ERC. The Korean Basic Science Institute is also acknowledged for allowing us to use transmission and scanning electron microscopes. The authors also want to express their gratitude to Seung-Kon Lee for the graphic artwork of the figures in this article.

References

- [1] Institute of Electrical and Electronics Engineers, IEEE C95.1-1991, IEEE standards for safety levels with respect to human exposure to radio frequency electromagnetic fields, 3 kHz to 300 GHz, New York, 1992.
- [2] Y. Ishihara, T. Hirai, C. Sakurai, T. Koyanagi, H. Nishida, M. Komatsu, *Thin Solid Films* 411 (2002) 50.
- [3] T. Inoue, T. Ishizaki, U.S. Patent No. 5831390, 3 Nov. 1998.
- [4] R.G. Gordon, *MRS Bull.* 25 (8) (2000) 52.
- [5] Y. Djaoued, V.H. Phong, S. Badile, *Thin Solid Films* 293 (1997) 108.
- [6] G. Kawachi, E. Kimura, Y. Wakui, N. Konoshi, H. Yamamoto, Y. Matsukawa, A. Sasano, *IEEE Trans. Electron. Devices* 41 (1994) 1120.
- [7] P. Stulik, J. Singh, *Sol. Energy Mater. Sol. Cells* 40 (1996) 239.
- [8] K. Molnar, T. Mohacsy, P. Varga, E. Vazsonyi, I. Barsony, *J. Lumin.* 80 (1999) 91.
- [9] D.M. Mattox, *Thin Solid Films* 204 (1991) 25.
- [10] J.J. Xu, A.S. Shaikh, R.W. Vest, *Thin Solid Films* 161 (1988) 273.
- [11] Y. Takahashi, S. Okada, R.B.H. Tahir, K. Nakano, T. Ban, Y. Ohya, *J. Non-Cryst. Solids* 218 (1997) 129.
- [12] M. Toki, M. Aizawa, *J. Sol–Gel Sci. Technol.* 8 (1997) 717.
- [13] A. Toufuku, K. Adachi, U. S. Patent No. 5,785,897, 28 Jul. 1998.
- [14] T. Morimoto, Y. Sanada, H. Tomonaga, *Thin Solid Films* 392 (2001) 214.
- [15] D.J. Kim, H. Kim, *J. Mater. Sci.* 33 (1998) 2931.
- [16] L. Wang, W. Sigmund, F. Aldinger, *J. Am. Chem. Soc.* 83 (4) (2000) 697.
- [17] H. Takeda, Y. Ohtsuka, K. Adachi, H. Kuno, European Patent Application 0779343A2, 18 Jun. 1997.
- [18] Z. Gao, Y. Gao, Y. Li, Y. Li, *Nanostruct. Mater.* 11 (5) (1999) 611.
- [19] B.D. Cullity, S.R. Stock, *Elements of X-ray Diffraction*, 3rd ed., Prentice Hall Inc, New Jersey, 2001, p. 167.
- [20] N. Yamada, I. Yasui, Y. Shigesato, H. Li, Y. Ujihira, K. Nomura, *Jpn. J. Appl. Phys.* 38 (1999) 2856.
- [21] C.A. Wah, L.Y. Choong, G.S. Neon, *Eur. Polym. J.* 36 (2000) 789.
- [22] H. Tomonaga, T. Morimoto, *Thin Solid Films* 392 (2001) 243.
- [23] K. Abe, Y.K. Sanada, T. Morimoto, *J. Sol–Gel Sci. Technol.* 22 (2001) 151.
- [24] W.B. Russel, D.A. Saville, W.R. Schowalter, *Colloidal Dispersion*, Cambridge University Press, New York, 1999, p. 189.